Computational Study of the Mechanisms for the Reaction of $O_2(^3\Sigma_g)$ with Aromatic Radicals

Cynthia Barckholtz, Michael J. Fadden, and Christopher M. Hadad*

Department of Chemistry, The Ohio State University, Columbus, Ohio 43210

Received: May 24, 1999; In Final Form: August 10, 1999

The potential energy surface (PES) of the $C_6H_5^\bullet + O_2(^3\Sigma_g)$ reaction has been studied using the B3LYP method. Several pathways were considered following the formation of the phenylperoxy ($C_6H_5OO^\bullet$) radical. At low temperatures ($T < 432$ K), the lowest energy pathway was found to go through a dioxiranyl radical. Scission of the O−O bond to form the phenoxy ($C_6H_5O^\bullet$) radical and $O(^3P)$ atom is more favorable at higher temperatures. Transition state structures for several steps in the decomposition of the phenylperoxy radical are presented to augment the $C_6H_5^\bullet + O_2$ PES. For the heteroatomic aromatic hydrocarbon radicals, such as pyridine, furan, and thiophene, only minima on the PES are calculated in analogy with the intermediates obtained for the reaction of phenyl radical with O_2. One important result of the proposed decomposition mechanism is that subsequent rearrangements of the heteroatomic aromatic hydrocarbon peroxy radicals (Ar−$OO^\bullet$) are likely to yield intermediates that are of atmospheric interest.

Introduction

There are several key reactions in the initial steps of the oxidation of benzene. Besides the attack on benzene by the radical pool of H, OH, and $O(^3P)$, another reaction that is significant in combustion is the subsequent reaction of the phenyl radical with molecular oxygen ($^3\Sigma_g$). This reaction is the source of many important intermediates in the oxidation of benzene. Several different reaction paths have been suggested and the array of possible products includes the cyclopentadienyl radical (Cp), CO, CO_2, O, and H.[1] Controversy exists over the dominant product channel as well as the mechanisms for the formation of these products.[2]

In contrast, the reactions of alkyl radicals with O_2 have been studied in greater detail.[3] The reaction of molecular oxygen with the vinyl radical ($C_2H_3^\bullet$) is the system that is most well correlated with the phenyl radical reaction. The primary products of this reaction have been experimentally shown to be CH_2O and $CHO^\bullet$ at temperatures below 1000 K.[4] At higher temperatures,[5] the dominant product channel is the formation of $C_2H_3O^\bullet + O$. Mechanisms to explain the products of the $C_2H_3^\bullet + O_2$ reaction both at low[6−8] and high temperatures[8] have been explored using ab initio methods. The proposed initial step in the oxidation of the vinyl radical for each of the suggested mechanisms is the formation of the vinylperoxy radical, $C_2H_3OO^\bullet$.

Similarly, the most frequently proposed mechanism for the low-temperature reaction of the phenyl radical ($C_6H_5^\bullet$) is the formation of the phenylperoxy radical

$$C_6H_5^\bullet + O_2 \rightarrow C_6H_5OO^\bullet \qquad (1)$$

as originally suggested by Norrish and Taylor.[9] They proposed that the phenylperoxy radical would react with another benzene molecule to form two very important intermediates, the phenoxy radical and phenol.

$$C_6H_5OO^\bullet + C_6H_6 \rightarrow C_6H_5O^\bullet + C_6H_5OH \qquad (2)$$

At high temperatures, however, it has been postulated that the phenylperoxy radical formed in reaction 1 will simply decompose back to reactants.[10] This argument is based on the estimation by Benson that the highest temperature at which bridged endoperoxide molecules formed from aromatic radicals are stable is ~600 K.[11] Therefore, another mechanism that leads directly to the formation of the phenoxy radical was proposed to be the key step in the oxidation of phenyl radical.[12]

$$C_6H_5^\bullet + O_2 \rightarrow C_6H_5O^\bullet + O^\bullet \qquad (3)$$

This reaction is favored because not only is it exothermic[13] by ~11 kcal·mol^{-1}, but it is also a chain propagation step as it leads to the formation of two radicals. In addition, the phenoxy radical can then thermally decompose to yield the $C_5H_5^\bullet$ (Cp) radical and CO, which are known to be products of the oxidation of benzene.

$$C_6H_5O^\bullet \rightarrow C_5H_5^\bullet + CO \qquad (4)$$

The mechanism for the subsequent thermal decomposition of the phenoxy radical has been extensively studied by ab initio methods.[14,15]

However, an experimental study of the reaction of $C_6H_5^\bullet$ with O_2 by cavity-ring down spectroscopy did not find evidence for the formation of the phenoxy radical at low temperatures.[16] Therefore, it was concluded that the reaction proceeds by an addition−stabilization channel to form the phenylperoxy radical at $T \leq 473$ K.

Carpenter has suggested an alternative pathway for the phenylperoxy decomposition that proceeds via a rearrangement pathway to form the phenyldioxiranyl radical rather than $C_6H_5O^\bullet$ and O.[6] Further rearrangement of the dioxiranyl radical yields the Cp radical and CO_2 as products. The key intermediates of this pathway were initially studied using the semi-empirical PM3 method.

Mebel and Lin have applied ab initio Hartree−Fock-based methods to study the isomers of $C_6H_5O_2^\bullet$[17] and the $C_6H_5O^\bullet$ +

10.1021/jp991692k CCC: $18.00
Published on Web 09/16/1999

O reaction.[18] On the basis of these calculations, several mechanisms for the reaction of $C_6H_5^\bullet$ with O_2 were postulated. These include scission of the O−O bond to form $C_6H_5O^\bullet$ and O, rearrangement to form the dioxiranyl radical followed by O-atom migration around the ring, and abstraction of an H atom from a neighboring carbon atom by the terminal O atom.

The work presented in this paper is an extension of the earlier calculations on the $C_6H_5^\bullet + O_2$ reaction. The density functional B3LYP method is used to assess the relative stability of the radicals formed after reaction 1. The free energies of the intermediates are calculated throughout the temperature range 298−2000 K to address the question of which mechanism is preferred at temperatures relevant to combustion. The oxidation pathways for several monocyclic aromatic radicals (pyridine, furan, and thiophene) were also surveyed (by calculation of dioxiranyl and peroxy radicals) to determine if the thermochemical calculations from the phenyl radical can be generalized to other heteroatomic aromatic radicals ($Ar^\bullet$). A subsequent paper will explore the PES, including transition states, for both the low- and high-temperature oxidation of these heteroatomic aromatic radicals.

Furthermore, low-temperature mechanisms are also important for reactions that occur following the release of combustion products into the atmosphere. Therefore, the thermal decomposition of the dioxiranyl radical, which is the most favorable pathway at low temperatures, is the focus of the remainder of this paper. Finally, the analogous mechanism is considered for several heteroatomic aromatic rings that represent functional groups known to be present in coal.

Computational Methods

The studies of the attack of molecular oxygen ($^3\Sigma_g$) on aryl radicals were performed using the hybrid density functional B3LYP method. This method has recently been shown to provide reliable energies for the potential energy surface of comparable model systems, including the calculation of C−H BDEs,[19] thermal decomposition pathways,[20] and O_2 oxidation.[21] One reason for the relative success of the B3LYP method compared to other inexpensive, unrestricted Hartree−Fock-based methods is that spin contamination is not a significant problem for the B3LYP wave functions. The $\langle S^2 \rangle$ value for the doublet species calculated by the B3LYP method for the aryl-based radicals in this paper ranged from a typical value of ∼0.75 to a maximum value of ∼0.79.

All geometry optimizations and frequency calculations were performed using Gaussian 94[22] at the Ohio Supercomputer Center. Geometries of each structure were fully optimized at the B3LYP/6-31G(d) level.[23−25] Cartesian coordinates of the reactants, products, intermediates, and transition states for the reaction mechanisms studied are available in the Supporting Information. Harmonic vibrational frequencies (also included in the Supporting Information) have also been calculated for each stationary point to verify the correct number of real and imaginary vibrational frequencies and to provide zero-point vibrational energy (ZPE) corrections, which were scaled by a factor of 0.9806.[26]

Transition states were confirmed to connect the desired reactants and products by incremental displacement of the coordinates from the transition state structure in each direction, followed by calculation of the analytical force constants and subsequent optimization.

The thermodynamic contributions to the enthalpy and free energy of each stationary point were obtained from the unscaled vibrational frequencies in order to calculate $\Delta H(T)$ and $\Delta G(T)$. A detailed description of the methods used to calculate the thermodynamic parameters, especially their temperature dependencies, has been described elsewhere.[27] Single point energies at the B3LYP/6-311+G(d,p)//B3LYP/6-31G(d) level, using six Cartesian *d* functions, were calculated to obtain more reliable energies for the PES.[19,28] Only these larger basis set free energies are discussed throughout the paper, but the smaller basis set results are presented in the Supporting Information.

Mechanism for the $Ar^\bullet + O_2$ Reaction

Relative Stability of Intermediates Formed from $C_6H_5OO^\bullet$. Oxidation of the phenyl radical via molecular oxygen ($^3\Sigma_g$) to form the phenylperoxy radical (reaction 1) is an energetically favorable reaction. The lowest energy conformation for the phenylperoxy radical has a planar, C_s geometry and has a $^2A''$ electronic ground state. The B3LYP/6-311+G(d,p)//B3LYP/6-31G(d) method calculates that this step is exoergic by ∼32.4 kcal·mol^{-1} at 298 K. The calculated ΔH of the reaction, 43.3 kcal·mol^{-1}, is in good agreement with the experimentally estimated exothermicity of ∼ 37 kcal·mol^{-1}.[29] A transition state for the formation of the peroxy radical from the reactants was not found. Transition state optimization attempts led to dissociation to form $C_6H_5^\bullet$ and O_2. This result is anticipated from related studies, which either assumed[5,30] the addition of O_2 to $C_2H_3^\bullet$ was barrierless or concluded from ab initio calculations[8] that the formation of the vinyl peroxy radical occurred without a barrier.

Further decomposition of the phenylperoxy radical was investigated along four major pathways. The calculated free energies (at 298 K) for the formation of the primary intermediate along each pathway are presented in Figure 1.

Path 1. Attack on the aromatic ring carbons by the terminal oxygen atom is one type of reaction that can occur in the decomposition process. In the phenylperoxy radical, the terminal oxygen atom has an interaction distance of 2.30 Å with carbon 1. The free energy penalty for rearrangement from the phenylperoxy radical to the most accessible intermediate, the dioxiranyl radical (1,1-addition), is 23.1 kcal·mol^{-1}. This intermediate, first proposed by Carpenter,[6] is less stable than the phenylperoxy radical due to the loss of aromaticity in the ring, although the unpaired electron is delocalized over the π system of the sp^2 carbons in the ring. The dioxiranyl radical has C_{2v} symmetry and a ground electronic state of $^2B_1$. The transition state for ring closure to form the dioxiranyl radical is calculated to be 27.2 kcal·mol^{-1} above the phenylperoxy radical.

Path 2. Scission of the O−O bond to form the phenoxy radical and an O atom is another available thermal decomposition pathway. This step is calculated to be endoergic by 27.7 kcal·mol^{-1}. However, the formation of the phenoxy radical directly from the attack of O_2 on the phenyl radical is still exoergic by ∼5 kcal·mol^{-1}. A transition state for the cleavage of the O−O bond could not be located at the B3LYP level. Spin contamination does become more severe ($\langle S^2 \rangle \sim 1.7$) as the O−O bond is stretched above 1.7 Å. Additional attempts at the CASSCF(7,7)/3-21G level have also been unsuccessful.

Although we cannot rule out the existence of the transition state for the reaction of $C_6H_5OO^\bullet \rightarrow C_6H_5O^\bullet + O^\bullet$, we have not been able to locate it. However, further insight into this path may also be gained from an earlier study of the vinyl radical + O_2.[8] In that study, an analagous transition state for the scission of the O−O bond was located. At the best level of theory used in the study, G2M(RCC,MP2), the transition state for formation of the vinyloxy ($C_2H_3O^\bullet$) radical (analogous to path 2) was 13.6 kcal·mol^{-1} higher than the barrier to form the dioxiranyl radical

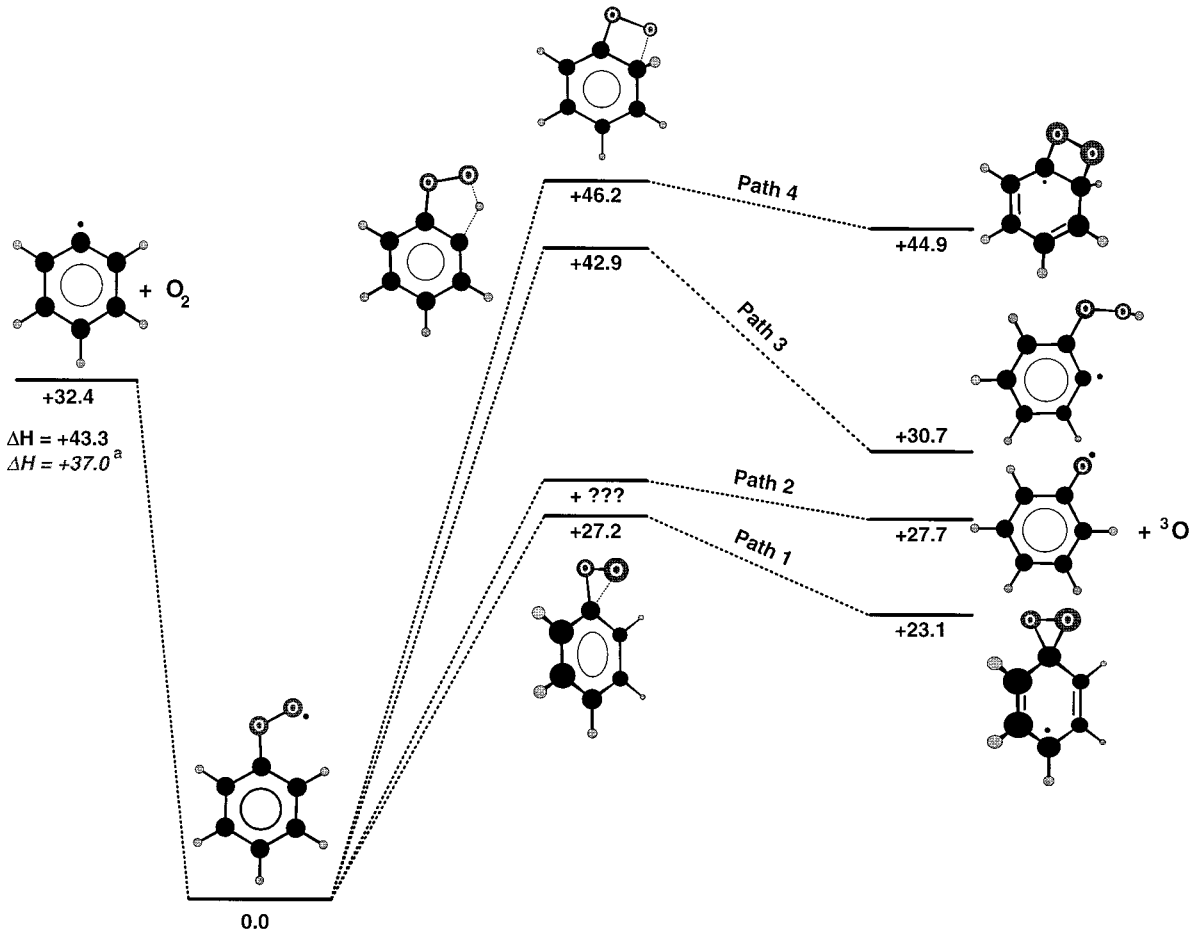

Figure 1. Four different pathways for the rearrangement of the phenylperoxy radical shown after O_2 attack on the phenyl radical. The free energy PES is calculated at the B3LYP/6-311+G(d,p)//B3LYP/6-31G(d) level of theory. Values are ΔG at 298 K, in kcal·mol^{-1}, except where noted. [a]Experimental estimate for ΔH_{298} is from ref 29.

(path 1) at 298 K. However, a near barrierless addition of O atom to CH_2CHO to form $C_2H_3OO^{\bullet}$ was found in a computational study of the analogous reverse reaction for path 2.[31]

Path 3. As a result of the short (2.41 Å) distance between the terminal oxygen and the ortho hydrogen atom in the phenylperoxy radical, another reaction pathway is available. Abstraction of a hydrogen atom from the ortho carbon atom by the terminal oxygen atom in phenylperoxy radical can lead to the formation of the ortho hydroperoxide phenyl radical. It has been suggested that the internal abstraction of an H atom is the most likely channel for the rearrangement of the vinylperoxy radical at higher temperatures.[32] For the phenyl radical, this H-atom migration pathway requires approximately the same overall energy as path 2. However, the transition state barrier to abstraction of the H atom by the terminal O atom is ~15.7 kcal·mol^{-1} higher than the barrier for path 1, reflecting the strength of an aryl C−H bond.[19]

Path 4. Rearrangement of the phenylperoxy radical can also occur if the terminal oxygen atom can add to one of its neighboring atoms. In the phenylperoxy radical, the terminal oxygen atom has an interaction distance of 2.72 Å with the ortho carbon. The cyclization to form a four-membered dioxetane ring (1,2-addition) is the most endoergic pathway considered here. The structure shown is for the case in which the O−O bond lies between the original radical carbon atom and the ortho carbon atom. This structure is analogous to the vinyldioxetanyl radical, which had been the mechanistic basis for vinyl radical oxidation[5] until Carpenter proposed the formation of a three-membered ring in a dioxiranyl radical.[6,7]

It can be seen in Figure 1 that there is a 21.8 kcal·mol^{-1} free energy preference for closure to form the dioxiranyl rather than the dioxetanyl ring. In addition, the activation barrier for the formation of the dioxetanyl radical is 19.0 kcal·mol^{-1} higher than the corresponding barrier for the formation of the dioxiranyl radical. Therefore, the B3LYP calculations suggest that the dioxiranyl radical should be an important intermediate in the oxidation of the phenyl radical.

Oxidation Pathway as a Function of Temperature. In order for computational chemistry to be useful as a predictive tool for the products of aromatic oxidation, it is necessary to discern the aromatic oxidation mechanism that is relevant over a particular temperature regime. The B3LYP calculations presented for the 298 K pathways for O_2 attack on the phenyl radical (Figure 1) can also be employed to predict pathways at higher temperatures by the inclusion of the enthalpy (ΔH) and entropy ($T\Delta S$) terms corresponding to the higher temperatures.

The free energies for the rearrangement of the phenylperoxy radical via the same paths illustrated in Figure 1 are shown in Figure 2 over the temperature range 298−2000 K. It is evident that at low temperatures the rearrangement from the phenylperoxy radical to form the dioxiranyl radical is the preferred mechanism. However, at temperatures greater than 432 K, the cleavage of the O−O bond to form the phenoxy radical and an oxygen atom is the thermodynamically preferred pathway. Moreover, the B3LYP calculations predict that, at temperatures greater than ~1196 K, it is unlikely that the phenylperoxy radical will form. Rather, formation of the phenoxy radical and an O atom (path 2) will occur directly, or the phenylperoxy radical

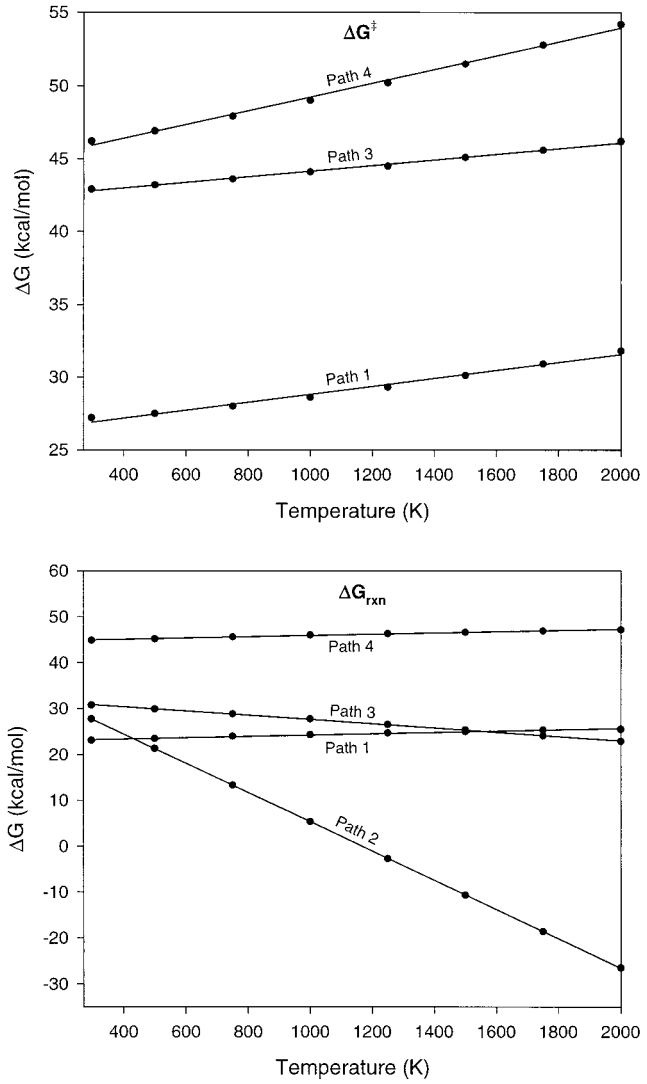

Figure 2. B3LYP/6-311+G(d,p)//B3LYP/6-31G(d) calculated transition state (top) and reaction (bottom) free energies for the rearrangement of the phenylperoxy radical to likely intermediates over the temperature range 298−2000 K.

will decompose back to reactants (phenyl radical and O_2). Other bimolecular reactions will then start to play a larger role.

There is experimental evidence to support the temperature dependence of the oxidation pathways predicted by computational chemistry. Cavity-ring down spectroscopy has been used for kinetic studies of the reaction of molecular oxygen with the phenyl radical by monitoring the presence of both the phenylperoxy and the phenoxy radicals.[16] These studies determined that at low temperatures ($T \leq 473$ K), the phenylperoxy radical is an important intermediate that leads to subsequent $C_6H_5O_2$ intermediates along the decomposition pathway. However, at high temperatures ($T \geq 1000$ K), the formation of the phenoxy radical via reaction 3 (path 2) dominates.[33] Therefore, at high temperatures, the mechanism for the oxidation of the phenyl radical would continue through the thermal decomposition of the phenoxy radical.[15]

Heteroatomic Aromatic Oxidation Pathways. The thermodynamics of the oxidation of several heteroatomic aromatic radicals was explored along the lower energy paths 1 and 2 to determine if the phenyl radical oxidation is a model reaction for other heteroatomic Ar• radicals. The room-temperature results are summarized in Table 1. At 298 K, there is an ∼4−5 kcal·mol^{-1} preference for the decomposition of the six-membered aryl peroxy radicals to occur via rearrangement to the dioxiranyl radical versus scission of the O−O bond.

TABLE 1: B3LYP/6-311+G(d,p)//B3LYP/6-31G(d) Free Energies (ΔG at 298 K, in kcal·mol^{-1}) for Rearrangement To Form the Dioxiranyl Radical (Path 1) and Scission of the O−O Bond (Path 2) Subsequent to O_2 Addition to Several Heteroatomic Aromatic Radicals

aryl radical	site	path 1	path 2
phenyl		+23.1	+27.7
pyridyl	2	+25.4	+30.5
	3	+22.1	+26.9
	4	+26.5	+31.5
furanyl	2	+5.5	+3.5
	3	+19.7	+20.4
thiophenyl	2	+9.1	+7.7
	3	+20.0	+21.8

The oxidation of the five-membered aryl peroxy radicals is not as straightforward. When the aryl peroxy radical is formed by O_2 addition at the 3-position of the five-membered rings, which is the site of the more stable aryl radical,[19] then there is a slight preference for path 1 over path 2. However, at the 2-position in furan and thiophene, the free energy penalty for decomposition of the peroxy radical to proceed along either path 1 or path 2 is significantly lower than the analogous step in six-membered arylperoxy radicals. One explanation for the relative stability of the dioxiranyl radical in the five-membered rings can be found in the optimized geometry of the dioxiranyl radicals. In the phenyldioxiranyl radical, the internal ring angle is ∼117° due to the geometric constraints of the planar six-membered ring. However, the hybridization of the dioxiranyl carbon atom is sp^3 and the structure would be lower in energy if the internal ring angle were closer to the tetrahedral angle of 109.5°. In contrast, the internal ring angle of the 2-furanyldioxiranyl radical is ∼ 107°, which is much closer to the preferred sp^3 angle.

Furthermore, scission of the O−O bond is the lower energy of the two pathways considered for the subsequent decomposition of the five-membered 2-arylperoxy radicals. To address the particular stability of the 2-aryloxy radicals, it is helpful to consider both the geometries and the resonance structures of representative five- and six-membered aryloxy radicals. In the six-membered aryloxy radicals studied, the B3LYP/6-31G(d) optimized geometries yield a C−O bond length of 1.25−1.26 Å. In contrast, aryloxy radicals formed at the 2-position in the five-membered rings have a C−O bond length of 1.21 Å. In general, the aryloxy C−O bond lengths are closer to that typical of C−O double bonds (1.20 Å) than C−O single bonds (1.43 Å).

However, the shorter C−O bond length in the five-membered 2-aryloxy radicals than in the six-membered analogues is evidence that the latter two resonance structures (II-B and II-C) of the five-membered 2-aryloxy radicals are more important

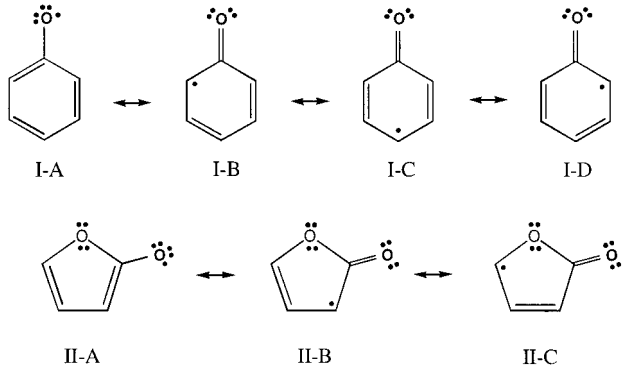

to describe the bonding than the latter three resonance structures (I-B, I-C, and I-D) of the six-membered aryloxy radicals. One explanation for the relatively greater contribution of these resonance structures in the 2-aryloxy radicals, which reflect the C−O double bond character, is that it is relatively easier to disrupt the aromatic ring π system in the five-membered rings than in the six-membered rings.[34] Therefore, the C−O bond exhibits more double bond character in the five-membered 2-aryloxy radicals than in the six-membered rings, which leads to a more stable aryloxy radical.

Only two resonance structures (III-A and III-B) can be drawn

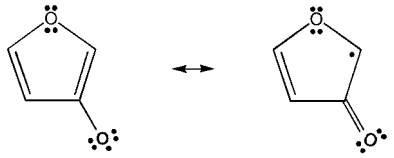

III-A III-B

for the five-membered aryloxy radicals at the 3-position. Since only III-B contributes C−O double character to the optimized geometry, it is not surprising that the C−O bond length (1.24 Å) in the five-membered 3-aryloxy radicals is greater than that of the five-membered 2-aryloxy radicals. As a result, the five-membered 3-aryloxy radicals are not as stable as the five-membered 2-aryloxy radicals, and the free energy required for scission of the O−O bond in the 3-peroxy radicals is ∼14−17 kcal·mol^{-1} greater than in the 2-peroxy radicals.

Unimolecular Decomposition Pathways to form CO and CO_2

Phenyl Radical Oxidation. The most probable mechanism that can be proposed for the low-temperature oxidation of the phenyl radical involves rearrangement of the phenylperoxy radical to form the dioxiranyl radical. Carpenter performed the first calculations for the subsequent mechanism, shown in Figure 3, at the PM3 level of theory.[6] Two ab initio methods, HF/6-31G(d) and B3LYP/6-311+G(d,p)//B3LYP/6-31G(d), have been used to calculate the phenyl oxidation path and are presented here. According to the proposed mechanism, thermal decomposition of the dioxiranyl radical (**3**) involves a concerted scission of the O−O bond and an exoergic (−71.1 kcal·mol^{-1}) rearrangement to form a very stable seven-membered ring (**5**). The formation of an oxirane ring (**4**) prior to the seven-membered ring was also postulated by Carpenter, but was not found to be a stationary point on the PM3 surface. However, structure **4** was calculated to be a local minimum on the HF surface, but not on the B3LYP surface. Spin contamination is a significant problem for the open-shell HF calculations, but is typically not a problem for the B3LYP calculations. Carpenter suggested that structure **5** is an important intermediate in the reaction of O_2 with the phenyl radical due to its relative stability. The location of the transition state that connects the dioxiranyl radical to the seven-membered ring has thus far been elusive. Therefore, further study of the formation of the seven-membered ring is warranted, and a complete analysis of the transition states for this PES will be presented in due course. The results presented here are thermodynamic estimates of the oxidation process.

Three possibilities were explored for the decomposition of structure **5**: a ring-opening reaction via C−O cleavage (**6**), expulsion of CO to form the pyranyl radical (**7**), and a cyclization reaction to structure **8**. All of the possibilities are energetically less favorable than the seven-membered ring, most likely due to decreased delocalization of the unpaired electron.

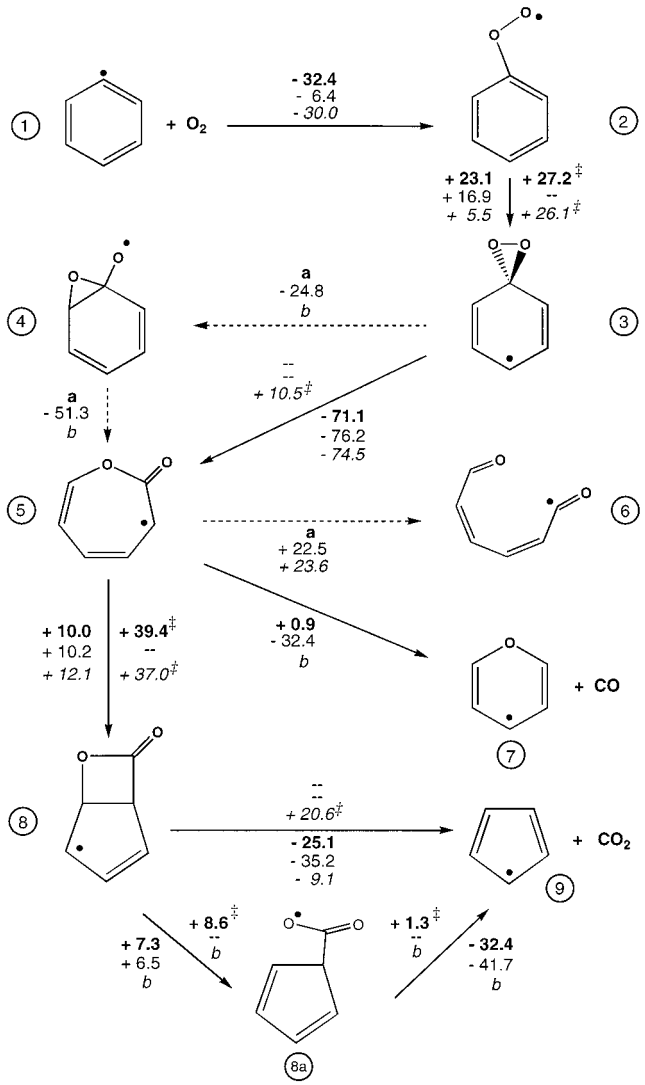

Figure 3. Reaction mechanism for the attack of O_2 on the phenyl radical at 298 K. Values are ΔG at the B3LYP/6-311+G(d,p)//B3LYP/6-31G(d) level (**bold**, top), ΔG at the HF/6-31G(d) level (normal, middle), and ΔH at the PM3 level (*italic*, bottom, from ref 6). Values marked with ‡ are free energy transition state barriers. All values are in kcal·mol^{-1}. [a]Not located as a minimum on the B3LYP surface. [b]Not calculated in ref 6.

Structure **6** was not found to be a minimum at the B3LYP/6-31G(d) level of theory. The second pathway, though not considered by Carpenter, is perhaps the most plausible because it is more energetically favorable. This pathway leads to the pyranyl radical (**7**) and CO. The net reaction free energy to form the pyranyl radical + CO from the phenyl radical and O_2 is −79.5 kcal·mol^{-1}.

Cyclization to form structure **8** occurs with a free energy penalty of 39.4 kcal·mol^{-1}. Stretching of the C−O bond in **8** opens the four-membered ring, with only a modest barrier of 8.6 kcal·mol^{-1}. Subsequent decomposition of **8a** leads to two experimentally known products of benzene oxidation, CO_2 and the Cp radical (**9**).[1,2] The **8a** → **9** reaction step is exoergic by 32.4 kcal·mol^{-1}, and the barrier is small, 1.3 kcal·mol^{-1}. The overall free energy for the reaction of $C_6H_5^{\bullet} + O_2 \rightarrow C_5H_5^{\bullet} + CO_2$ is −108.1 kcal·mol^{-1}. While the reaction of the phenyl radical with O_2 is a multistep process, the majority of the net exoergicity is a result of two of the steps: the initial formation of the phenylperoxy radical (**2**) and the rearrangement of the dioxiranyl radical (**3**) to form the seven-membered ring (**5**).

Pyridyl Radical Oxidation. There has been much effort to elucidate the mechanism for the oxidation of aromatic hydrocarbons. However, very little is known about the oxidation of heteroatomic aromatic compounds, particularly those that contain nitrogen and sulfur atoms. [35] It is important to study the pyrolysis and oxidation of heteroatomic aromatic compounds because these can model the reactions that occur for nonpetroleum fuels, such as coal. For example, an understanding of the formation and consumption of nitrogen-containing species during the combustion of fuel nitrogen has important implications for the control of nitrogen oxide (NO_x) emissions from a coal-fired power plant.

There are three sources of NO_x from the combustion process:[36] (1) "thermal" NO_x, which is created via the reaction of atmospheric N_2 and O_2 at the high temperatures of the combustion process; (2) "prompt" NO_x, which is generated via the reactions of hydrocarbon free radicals with N_2; and (3) "fuel" NO_x, which is released by the oxidation and pyrolysis of nitrogen-containing organic compounds within the fuel macrostructure. Of these three, the principal source of NO_x from the combustion of nonpetroleum fuels is the fuel NO_x source.

There have recently been several significant contributions to understanding the mechanism by which nitrogen-containing heterocyclic aromatic compounds react under pyrolysis conditions.[35−43] Experimental evidence from the high-temperature pyrolysis of model nitrogen-containing aromatic compounds, such as pyridine,[36−38,44] suggests that the dominant nitrogen-containing product is hydrogen cyanide, HCN, which is a major precursor to the formation of NO_x. Rupture of the aromatic ring at the heterocyclic site has been proposed as the mechanism that leads directly to HCN formation in a pyrolytic environment.[36] In addition, the nitrogen-containing species observed from the pyrolysis of pyridine in the presence of oxygen were found to be the same—namely, HCN continued to be the major product.[35] However, very little is known about the mechanism by which nitrogen-containing aromatic compounds such as pyridine react under oxidation conditions.

The mechanism for the oxidation of the phenyl radical can serve as a foundation for understanding the oxidation of other monocyclic heteroatomic aromatic radicals. A mechanism for the oxidation of pyridine at 298 K, analogous to the phenyl oxidation mechanism (Figure 3), is presented in Figure 4. All structures shown are intermediates that have been calculated at the B3LYP/6-311+G(d,p)//B3LYP/6-31G(d) level of theory (transition states for such a mechanism will be presented in due course). This mechanism starts with the attack of molecular oxygen on the 2-pyridyl radical. This particular example was chosen due to the relative ease with which a hydrogen atom is removed from the 2-position of pyridine to form the 2-pyridyl radical compared to the 3- or 4-pyridyl radicals.[19,27]

Rearrangement following formation of the pyridylperoxy radical (**11**) leads to the pyridyldioxiranyl radical (**12**). The free energies of these two steps are very similar to those for the oxidation of the phenyl radical. However, due to the reduced symmetry caused by the nitrogen atom, there are now two possible pathways for further unimolecular decomposition. It is energetically favorable in both instances to form a seven-membered ring, but rearrangement along path B gives rise to a heteroatomic radical that has a nitrogen atom adjacent to an oxygen atom (structure **13b**), which is relatively less stable than structure **13a**, which does not have a N−O bond. Expulsion of CO from **13a** is ∼30 kcal·mol^{-1} more endoergic than expulsion of CO from **13b** due to the formation of a six-membered ring with adjacent nitrogen and oxygen atoms. However, given the exoergicity of the previous step (∼73 kcal·mol^{-1}), this step is quite feasible and leads to subsequent expulsion of HCN, a precursor to the formation of NO_x. As an alternative to the expulsion of CO from **13a** or **13b**, these seven-membered rings can rearrange to structures **16a** and **16b**, respectively, which are similar to **8** from the oxidation of the phenyl radical. These structures lead to the expulsion of CO_2 and the N-pyrrolyl radical (**17**), which is analogous to the Cp radical. The structure **16b** optimizes to a single ring structure prior to CO_2 expulsion along path B since it is unfavorable to have adjacent nitrogen and oxygen atoms in the bicyclic ring structure.

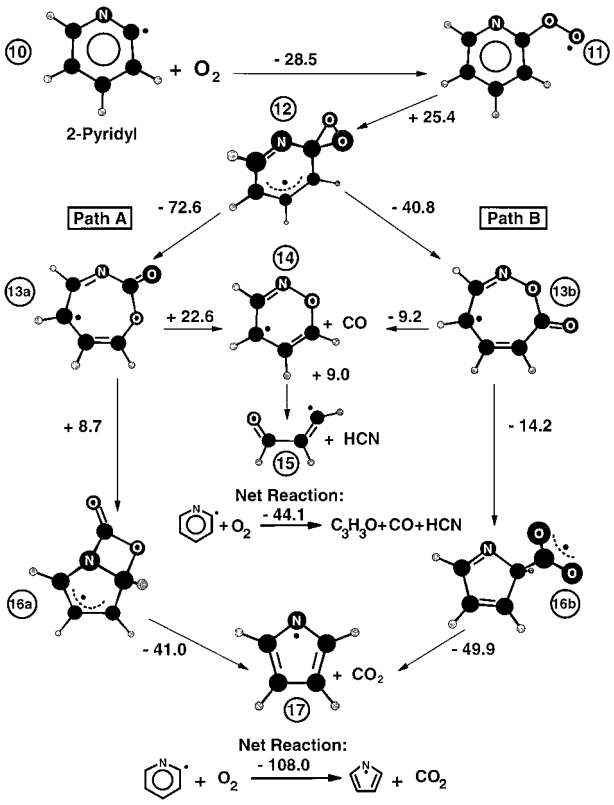

Figure 4. Reaction mechanism for the attack of O_2 on the 2-pyridyl radical at 298 K. All values are ΔG at the B3LYP/6-311+G(d,p)//B3LYP/6-31G(d) level of theory, in kcal·mol^{-1}.

It is evident from a comparison between Figures 3 and 4 that the oxidation process for the phenyl and pyridyl radicals is energetically quite similar, though there are more possible intermediates formed from the decomposition of the pyridylperoxy radical. There also exists an energetically feasible path for the formation of HCN following cleavage of the O−N bond. It has been suggested that at high temperatures pyrrole is even less stable than pyridine and leads even more readily to the production of NO_x via HCN.[36]

Furanyl Radical Oxidation. Furan is one of the most important oxygen-containing aromatic compounds that is a known intermediate in the combustion of coal.[45] The investigations into the chemical reactions of furan that are relevant to the burning of fossil fuels have focused on either the thermal decomposition[46−48] of furan or the subsequent reactions of furan with species of atmospheric interest.[49−54] Mechanisms for the oxidation of furan, however, have received little attention. There is very little preference (0.1 kcal·mol^{-1}) for the formation of the 3-furanyl over the 2-furanyl radical.[19] Therefore, it is necessary to study the oxidation pathways available to both radicals. Mechanisms analogous to that for phenyl oxidation

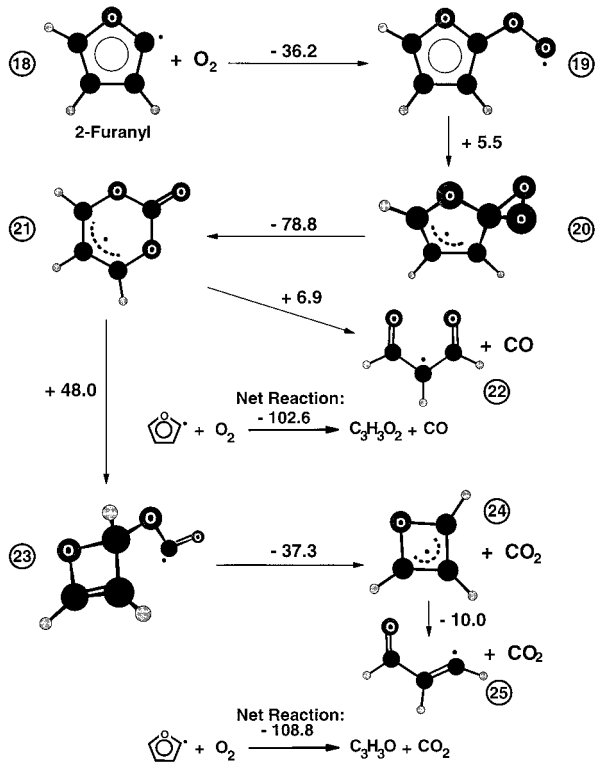

Figure 5. Reaction mechanism for the attack of O_2 on the 2-furanyl radical at 298 K. All values are ΔG at the B3LYP/6-311+G(d,p)// B3LYP/6-31G(d) level of theory, in kcal·mol^{-1}.

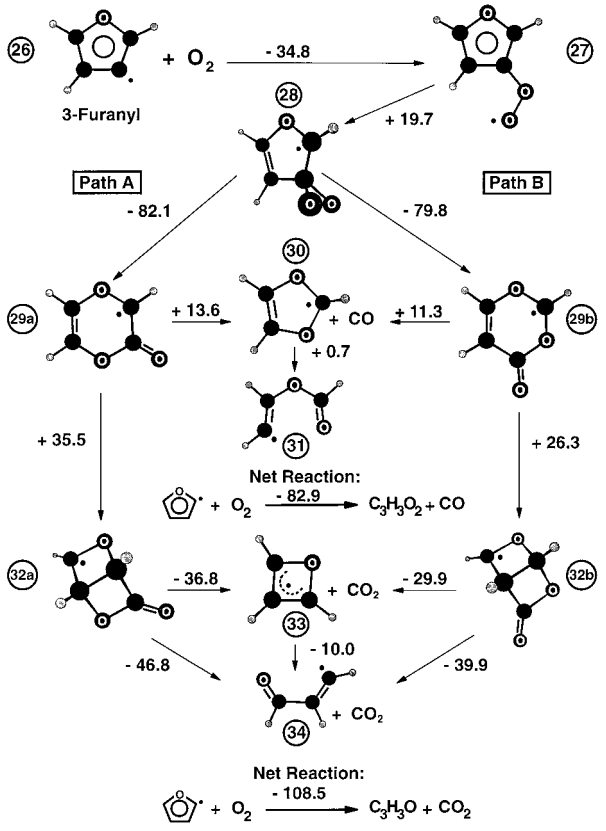

Figure 6. Reaction mechanism for the attack of O_2 on the 3-furanyl radical at 298 K. All values are ΔG at the B3LYP/6-311+G(d,p)// B3LYP/6-31G(d) level of theory, in kcal·mol^{-1}.

have been calculated using the B3LYP method and are shown for the 2-furanyl and the 3-furanyl radicals in Figures 5 and 6, respectively.

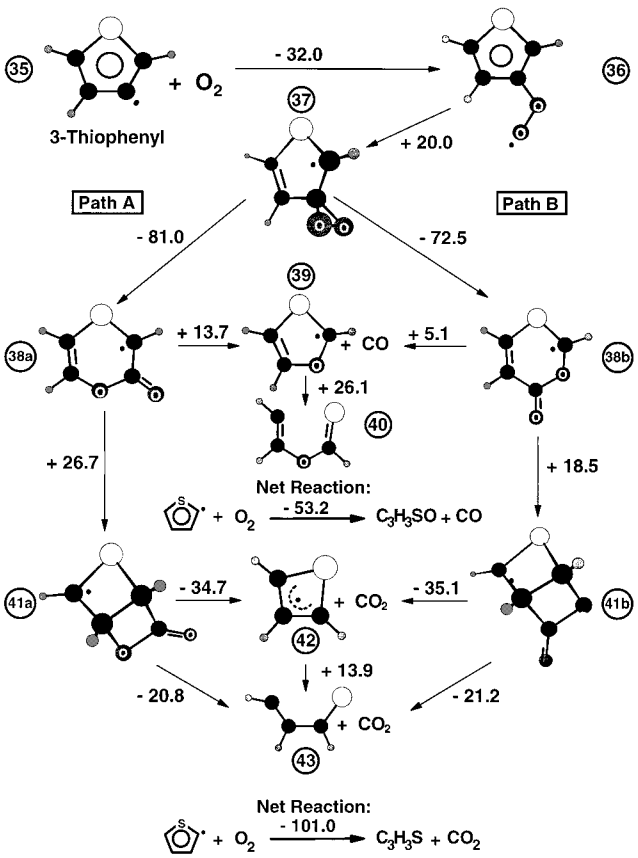

Figure 7. Reaction mechanism for the attack of O_2 on the 3-thiophenyl radical at 298 K. All values are ΔG at the B3LYP/6-311+G(d,p)// B3LYP/6-31G(d) level of theory, in kcal·mol^{-1}.

The attack of O_2 on each of the furanyl radicals to form the furanylperoxy radicals occurs with approximately the same free energy release as for reactions of the phenyl and 2-pyridyl radicals with O_2. It can be seen in Figure 5, however, that the free energy penalty for rearrangement to form the dioxiranyl radical (**20**) is much lower (~5.5 kcal·mol^{-1}) for the 2-furanyl radical than for any of the aromatic radicals studied to date. The subsequent rearrangement of the dioxiranyl radical to form a six-membered ring (**21**) with a carbonate functionality is very favorable energetically, similar to the stabilizing effect of forming a seven-membered ring that was evident in the phenyl and 2-pyridyl radical cases. Expulsion of CO from the six-membered ring to form a resonance-stabilized glyoxal radical (**22**) is the most accessible pathway. However, rearrangement that eventually leads to the loss of CO_2 and the formation of an acrolein radical (**25**) is also an accessible pathway.

Oxidation of the 3-furanyl radical can occur by a similar pathway. It is evident from a comparison between Figures 5 and 6 that there is a greater preference for loss of CO from the six-membered ring versus loss of CO_2 in the oxidation of the 2-furanyl radical than in the oxidation of the 3-furanyl radical. The bicyclic radicals (**32a** and **32b**) were calculated to be minima for both of the pathways available in the unimolecular decomposition from the six-membered rings (**29a** and **29b**). It is also striking that products formed by the furanyl oxidation mechanism leading to the formation of CO_2 (**25** and **34**) are the same regardless of the site of O_2 attack. Finally, it is noteworthy that the products formed via oxidation of furanyl radical, $C_3H_3O_2^{\bullet}$ (**22** and **31**) and CO or $C_3H_3O^{\bullet}$ (**25** and **34**) and CO_2, are quite similar to the known products of the thermal decomposition (without oxygen) of furan: propyne (C_3H_4) and CO.[47,48]

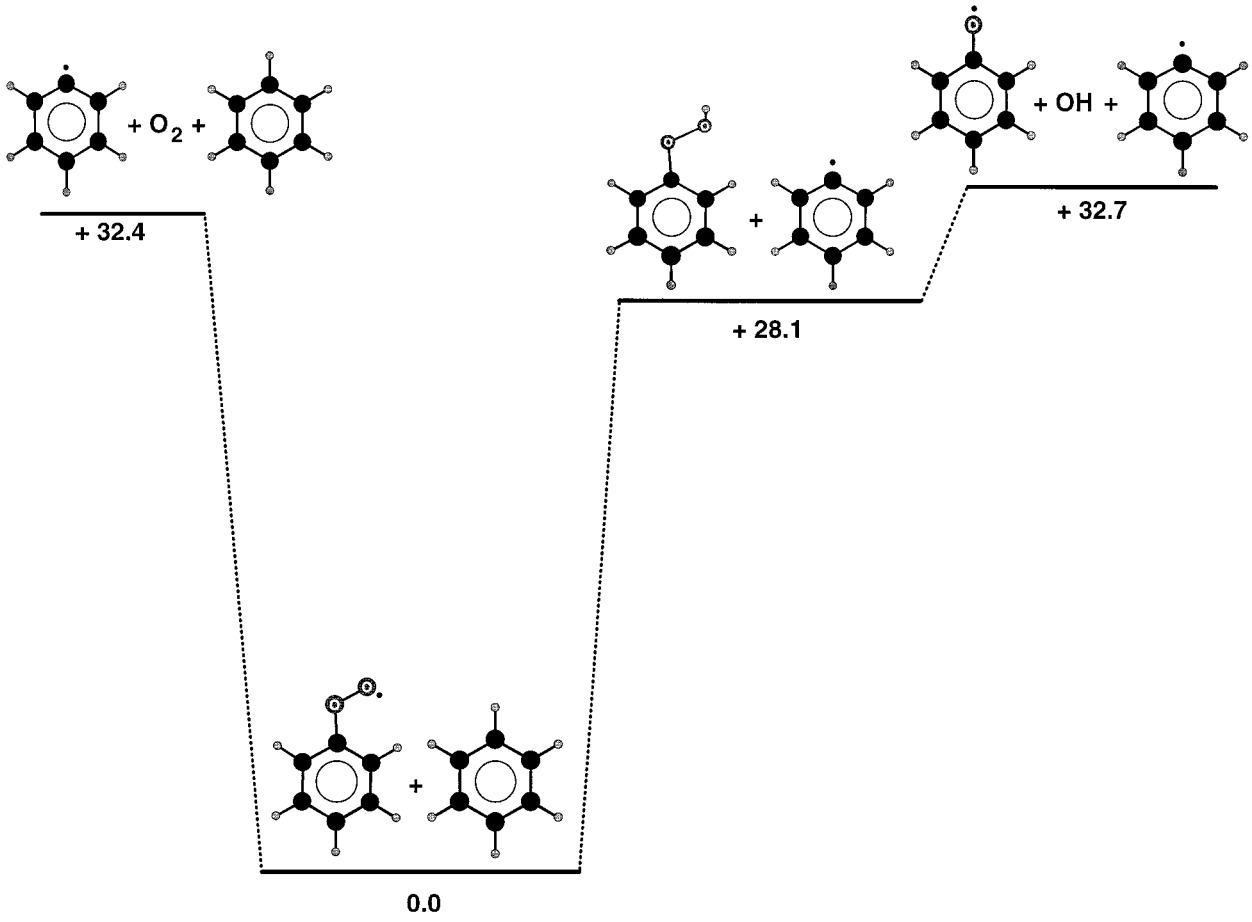

Figure 8. B3LYP/6-311+G(d,p)//B3LYP/6-31G(d) reaction free energies (at 298 K, in kcal·mol^{-1}) for the formation of the phenoxy radical via the bimolecular reaction of the phenylperoxy radical with benzene.

Thiophenyl Oxidation. The thiophene ring is an important component in coal that gives rise to the release of numerous sulfur-containing organic compounds into the atmosphere as a result of coal combustion and processing. The same mechanism for the oxidation of aromatic radicals at low temperatures was also applied to the 3-thiophenyl radical and is shown in Figure 7. The 3-thiophenyl radical was chosen to illustrate the oxidation of thiophene due to the ~3 kcal·mol^{-1} preference for the formation of the radical at the 3-position over the 2-position.[19,27] The reaction free energies for the thiophenyl pathway are quite similar to that of the 3-furanyl pathways and therefore will not be discussed further.

Comparison of Oxidation Pathway Energetics. It is evident from a comparison of the oxidation of several aromatic radicals via the dioxiranyl intermediate (Figures 3−7) that the free energies to form the analogous intermediates are approximately the same. This point is further illustrated in the summary of the free energies for the first several oxidation steps (Table 2). The free energies for the formation of the peroxy radicals and subsequent rearrangement to form the dioxiranyl radicals and then the expanded ring are quite similar. (Explanations for the exceptions have been offered earlier.) The net reaction free energies for the formation of Cp (and analogues) and CO_2 are also quite comparable. In fact, the net reaction free energies of the phenyl, 2-pyridyl, and 2- and 3-furanyl radicals are within 1 kcal·mol^{-1} of each other. One distinction between the oxidation pathways of the furanyl and thiophenyl radicals is the geometry of the lowest energy intermediates that are formed at the end of the pathway. A ring-opened radical is preferentially formed accompanying expulsion of CO_2 or formed at a small free energy penalty accompanying expulsion of CO from the furanyl radicals. The lowest energy configurations for the analogous intermediates formed from the 3-thiophenyl radical are closed rings.

TABLE 2: Comparison of Free Energies for the Initial, Individual Steps of the Low-Temperature Aryl Radical Oxidation Mechanism[a]

aryl radical	site	peroxy radical	dioxiranyl radical	expanded ring path A	expanded ring path B
phenyl		−32.4	+23.1	−71.1	
pyridyl	2	−28.5	+25.4	−72.6	−40.8
	3	−30.4	+22.1	−76.5	−68.2
	4	−30.4	+26.5	−72.2	
furanyl	2	−36.2	+5.5	−78.8	
	3	−34.8	+19.7	−82.1	−79.8
thiophenyl	2	−32.0	+9.1	−78.0	
	3	−32.0	+20.0	−81.0	−72.5

[a] Column titles represent the product formed in that step. Free energies of reaction (298 K, kcal·mol^{-1}) are at the B3LYP/6-311+G(d,p)//B3LYP/6-31G(d) level of theory.

Bimolecular Reactions Relevant to Phenyl Oxidation

The reaction of the phenyl radical with O_2 gives various products including several that have already been discussed, such as the Cp radical, CO_2, and CO, as well as oxygen and hydrogen atoms.[10,29,55] However, the oxidation pathway illustrated in Figure 3 does not lead directly to the appearance of oxygen and hydrogen atoms. Therefore, it has generally been thought that the decomposition path of phenylperoxy radicals

proceeds via scission of the O−O bond (path 2) to account for the observed O atoms as well as to be a source of phenoxy radicals (reaction 3).[10] However, it has been estimated that this reaction only accounts for ∼14% of the formation of the phenoxy radical.[2] Since it is accepted that the main oxidative decomposition of benzene or the phenyl radical (under combustion conditions) involves the phenoxy radical,[10] it is necessary to consider reactions other than reaction 3 that can lead to the phenoxy radical. Other reactions that have been proposed for the formation of the phenoxy radical[10] include the addition reaction

$$C_6H_5^{\bullet} + O \rightarrow C_6H_5O^{\bullet} \qquad \Delta G = -117.2 \text{ kcal·mol}^{-1} \quad (5)$$

the addition−elimination reaction

$$C_6H_6 + O \rightarrow C_6H_5O^{\bullet} + H^{\bullet} \qquad \Delta G = -7.8 \text{ kcal·mol}^{-1} \quad (6)$$

and the two-step reaction of the phenyl radical with HO_2 to yield phenoxy and hydroxyl radicals:

$$C_6H_5^{\bullet} + HO_2^{\bullet} \rightarrow C_6H_5OOH \qquad \Delta G = -66.3 \text{ kcal·mol}^{-1} \quad (7)$$

$$C_6H_5OOH \rightarrow C_6H_5O^{\bullet} + OH^{\bullet} \qquad \Delta G = +10.6 \text{ kcal·mol}^{-1} \quad (8)$$

The original Norrish and Taylor proposal[9] is quite similar to reaction 6 and involves species that are in high concentrations in the combustion process. This scheme, shown in Figure 8, involves the reaction of a phenylperoxy radical with another benzene molecule. In a propagation step, the peroxy radical abstracts a hydrogen atom from the benzene radical to form a phenyl radical and phenyl hydroperoxide. Two reactive species are generated via subsequent scission of the peroxide O−O bond—the phenoxy radical and an OH radical—though at a free energy penalty of ∼5.3 kcal·mol^{-1}.

Conclusions

Several mechanisms for the decomposition of aromatic compounds have been discussed in this paper. The reactions of the phenyl radical were explored in particular detail as the phenyl radical serves as the model from which the oxidation of other heteroatomic aromatic radicals can be considered. Oxidation mechanisms have been calculated at temperatures relevant to both atmospheric and combustion processes. The thermodynamic information for the unimolecular decomposition pathways of the heteroatomic aromatic radicals (derived from pyridine, furan, and thiophene) are intended to serve as foundations for further computational study of the oxidation pathways available to functional groups that are present in coal.

Acknowledgment. We gratefully acknowledge the U.S. Department of Energy (Grant DE-FG22-96PC96249) and the Ohio Supercomputer Center for support of this research. We thank Timothy A. Barckholtz for valuable discussions. Also, we thank Robert Essenhigh (The Ohio State University), Robert Hurt (Brown University), and Joseph Calo (Brown University) for helpful conversations.

Supporting Information Available: Energies for the intermediates of the reaction of O_2 with phenyl, 2-pyridyl, 2-furanyl, 3-furanyl, and 3-thiophenyl (pages S3−S5); energies for peroxy radicals (page S6), dioxiranyl radicals (page S7), expanded ring radicals (page S8), and phenoxy analogue radicals (page S8); and free energies for the rearrangement pathways of the phenylperoxy radical as a function of temperature (page S8). Reaction mechanisms for the oxidation of phenyl, 2-pyridyl, 2- and 3-furanyl, and 3-thiophenyl radicals at the B3LYP/6-31G(d) level of theory (pages S9−S13). Cartesian coordinates (page S14−S20) and harmonic vibrational frequencies (pages S21−S27) for the reactants, products, intermediates, and transition state structures for phenyl, 2-pyridyl, 2- and 3-furanyl, and 3-thiophenyl reactions with O_2. This material is available free of charge via the Internet at http://pubs.acs.org.

References and Notes

(1) Bittker, D. A. *Combust. Sci. Technol.* **1991**, *79*, 49−72.
(2) Zhang, H.-Y.; McKinnon, J. T. *Combust. Sci. Technol.* **1995**, *107*, 261−300.
(3) Hucknall, K. J. *Chemistry of Hydrocarbon Combustion*; Chapman and Hall: New York, 1985.
(4) Slagle, I. R.; Park, J.-Y.; Heaven, M. C.; Gutman, D. *J. Am. Chem. Soc.* **1984**, *106*, 4356−4361.
(5) Bozzelli, J. W.; Dean, A. M. *J. Phys. Chem.* **1993**, *97*, 4427−4441.
(6) Carpenter, B. K. *J. Am. Chem. Soc.* **1993**, *115*, 9806−9807.
(7) Carpenter, B. K. *J. Phys. Chem.* **1995**, *99*, 9801−9810.
(8) Mebel, A. M.; Diau, E. W. G.; Lin, M. C.; Morokuma, K. *J. Am. Chem. Soc.* **1996**, *118*, 9759−9771.
(9) Norrish, R. G. W.; Taylor, G. W. *Proc. R. Soc.* **1956**, *A234*, 160−177.
(10) Brezinsky, K. *Prog. Energy Combust. Sci.* **1986**, *12*, 1−24.
(11) Benson, S. W. *J. Am. Chem. Soc.* **1965**, *87*, 972.
(12) Westbook, C. K.; Dryer, F. L. *Prog. Energy Combust. Sci.* **1984**, *10*, 1−57.
(13) Benson, S. W. *Thermochemical Kinetics*, 2nd ed.; John Wiley and Sons: New York, 1976.
(14) Olivella, S.; Sole, A.; Garcia-Raso, A. *J. Phys. Chem.* **1995**, *99*, 10549−10556.
(15) Liu, R.; Morokuma, K.; Mebel, A. M.; Lin, M. C. *J. Phys. Chem.* **1996**, *100*, 9314−9322.
(16) Yu, T.; Lin, M. C. *J. Am. Chem. Soc.* **1994**, *116*, 9571−9576.
(17) Mebel, A. M.; Lin, M. C. *J. Am. Chem. Soc.* **1994**, *116*, 9577−9584.
(18) Lin, M. C.; Mebel, A. M. *J. Phys. Org. Chem.* **1995**, *8*, 407−420.
(19) Barckholtz, C.; Barckholtz, T. A.; Hadad, C. M. *J. Am. Chem. Soc.* **1999**, *121*, 491−500.
(20) Bacskay, G. B.; Martoprawiro, M.; Mackie, J. C. *Chem. Phys. Lett.* **1999**, *300*, 321−330.
(21) Ghigo, G.; Tonachini, G. *J. Chem. Phys.* **1999**, *110*, 7298−7304.
(22) Frisch, M. J.; Trucks, G. W.; Schlegel, H. B.; Gill, P. M. W.; Johnson, B. G.; Robb, M. A.; Cheeseman, J. R.; Keith, T.; Petersson, G. A.; Montgomery, J. A.; Raghavachari, K.; Al-Laham, M. A.; Zakrzewski, V. G.; Ortiz, J. V.; Foresman, J. B.; Cioslowski, J.; Stefanov, B. B.; Nanayakkara, A.; Challacombe, M.; Peng, C. Y.; Ayala, P. Y.; Chen, W.; Wong, M. W.; Andres, J. L.; Replogle, E. S.; Gomperts, R.; Martin, R. L.; Fox, D. J.; Binkley, J. S.; Defrees, D. J.; Baker, J.; Stewart, J. J. P.; Head-Gordon, M.; Gonzalez, C.; Pople, J. A. *Gaussian 94*, Revision C.3.; Gaussian, Inc.: Pittsburgh, PA, 1995.
(23) Becke, A. D. *Phys. Rev. A* **1988**, *38*, 3098−3100.
(24) Lee, C.; Yang, W.; Parr, R. G. *Phys. Rev. B* **1988**, *37*, 785−789.
(25) Hehre, W. J.; Radom, L.; Schleyer, P. v. R.; Pople, J. A. *Ab Initio Molecular Orbital Theory*; John Wiley & Sons: New York, 1986.
(26) Scott, A. P.; Radom, L. *J. Phys. Chem.* **1996**, *100*, 16502−16513.
(27) Barckholtz, C.; Hadad, C. M., to be submitted.
(28) Bauschlicher, Jr., C. W.; Langhoff, S. R. *Mol. Phys.* **1999**, *96*, 471−476.
(29) Lin, C.-Y. Ph.D. The Catholic University of America, 1987.
(30) Westmoreland, P. R. *Combust. Sci. Technol.* **1992**, *82*, 151−168.
(31) As cited in: Knyazev, V. D.; Slagle, I. R.. *J. Phys. Chem.* **1995**, *99*, 2247−2249.
(32) Knyazev, V. D.; Slagle, I. R. *J. Phys. Chem. A* **1998**, *102*, 1770−1778.
(33) Lin, C. Y.; Lin, M. C. *J. Phys. Chem.* **1986**, *90*, 425−431.
(34) Garratt, P. J. *Aromaticity*; Wiley: New York, 1986.
(35) Lifshitz, A. *Combust. Flame* **1989**, *78*, 43−57.
(36) Nimmo, W.; Richardson, J.; Hampartsoumian, E. *J. Inst. Energy* **1995**, *68*, 170−177.
(37) Mackie, J. C.; Colket III, M. B.; Nelson, P. F. *J. Phys. Chem.* **1990**, *94*, 4099−4106.
(38) Kiefer, J. H.; Zhang, Q.; Kern, R. D.; Yao, J.; Jursic, B. *J. Phys. Chem. A* **1997**, *101*, 7061−7073.

(39) Lifshitz, A.; Tamburu, C.; Suslensky, A. *J. Phys. Chem.* **1989**, *93*, 5802−5808.
(40) Laskin, A.; Lifshitz, A. *J. Phys. Chem. A* **1998**, *102*, 928−946.
(41) Doughty, A.; Mackie, J. C. *J. Chem. Soc., Faraday Trans.* **1994**, *90*, 541−548.
(42) Cullis, C. F.; Norris, A. C. *Carbon* **1972**, *10*, 525−537.
(43) Laskin, A.; Lifshitz, A. *J. Phys. Chem. A* **1997**, *101*, 7787−7801.
(44) Williams, A.; Pourkashanian, M.; Jones, J. M.; Rowlands, L. *J. Inst. Energy* **1997**, *70*, 102−113.
(45) Pellizzari, E. D.; Bunch, J. E.; Berkeley, R. E.; McRaie, J. *Anal. Chem.* **1976**, *48*, 803−807.
(46) Grela, M. A.; Amorbieta, V. T.; Colussi, A. J. *J. Phys. Chem.* **1985**, *89*, 38−41.
(47) Lifshitz, A.; Bidani, M.; Bidani, S. *J. Phys. Chem.* **1986**, *90*, 5373−5377.
(48) Organ, P. P.; Mackie, J. C. *J. Chem. Soc., Faraday Trans.* **1991**, *87*, 815−823.
(49) Atkinson, R.; Aschmann, S. M.; Carter, W. P. L. *Int. J. Chem. Kinet.* **1983**, *15*, 51−61.
(50) Bierbach, A.; Barnes, I.; Becker, K. H. *Atmos. Environ.* **1992**, *26A*, 813−817.
(51) Bierbach, A.; Barnes, I.; Becker, K. H. *Atmos. Environ.* **1995**, *29*, 2651−2660.
(52) Lee, J. H.; Tang, I. N. *J. Chem. Phys.* **1982**, *77*, 4459−4463.
(53) Wine, P. H.; Thompson, R. J. *Int. J. Chem. Kinet.* **1984**, *16*, 867−878.
(54) Tabares, F. L.; Urena, A. G. *J. Chem. Soc., Faraday Trans. 2* **1985**, *81*, 1395−1405.
(55) Glassman, I. *Combustion*; Academic Press: San Diego, 1996.